Cooperative doping effects of Ti and C on critical current density and irreversibility field of MgB_2

Y. Zhao[a)]
Key Laboratory of Advanced Technologies of Materials (Ministry of Education of China), Superconductivity R&D Center (SRDC), Southwest Jiaotong University, Sichuan 610031, China and School of Materials Science and Engineering, University of New South Wales, Sydney, 2052 New South Wales, Australia

Y. Feng
Northwest Institute for Nonferrous Metal Research, P.O. Box 51, Xi'an, Shaanxi 710016, China

T. M. Shen, G. Li, and Y. Yang
Key Laboratory of Advanced Technologies of Materials (Ministry of Education of China), Superconductivity R&D Center (SRDC), Southwest Jiaotong University, Sichuan 610031, China

C. H. Cheng
School of Materials Science and Engineering, University of New South Wales, Sydney, 2052 New South Wales, Australia

(Received 16 August 2006; accepted 15 October 2006; published online 19 December 2006)

Carbon and titanium concurrently doped MgB_2 alloys with a composition of $Mg_{1-x}Ti_xB_{2-y}C_y$ have been prepared by an *in situ* solid state reaction method. The combination effects of carbon and Ti doping on structure, microstructure, irreversibility field (H_{irr}), and critical current density (J_c) of MgB_2 have been investigated. It is found that doping Ti in MgB_2 does not reduce the solubility of carbon in MgB_2, but, on the contrary, it eliminates the porosity present in the carbon-doped MgB_2, resulting in an improved intergrain connectivity. As a result, J_c and H_{irr} of MgB_2 have been significantly improved, sharply contrasted to the situation of C-only-doped or Ti-only-doped MgB_2 bulks. Our results clearly reveal that carbon and Ti codoping are largely cooperative in improving the performance of MgB_2 in the high magnetic fields (>3 T) and at high temperature (~20 K).
 [DOI: 10.1063/1.2402963]

I. INTRODUCTION

The discovery of superconductivity at 39 K in MgB_2 offers the possibility of wide engineering applications in a temperature range of 20–30 K, where the conventional superconductors, such as Nb_3Sn and Nb–Ti alloy, cannot play any roles because of low T_c. However, so far, the applications of MgB_2 are hampered by its poor mechanical properties (brittleness) and the degradation of J_c in high magnetic fields. Great effort has been done to improve the critical field and current-carried ability of MgB_2 superconducting materials. Among many methods, alloying with carbon seems to be the most effective to improve the H_{c2} by shortening the mean free length of electron, or selective tuning of impurity scattering of π and σ bands according to the two-gap model of H_{c2} of Gurevich.[1,2] Recently, Braccini *et al.*[3] reported $H_{c2}(0)^{\parallel} > 50$ T for C-doped MgB_2 films. Fits to the data showed an extrapolated $H_{c2}(0)^{\parallel}$ (H parallel to the Mg and B planes) of ~70 T and $H_{c2}(0)^{\perp}$ exceeding 40 T. Such critical field exceeds those of any Nb-based conductor at any temperature, suggesting that MgB_2 could be a feasible replacement for Nb_3Sn as a high field magnet conductor. For untextured carbon-doped filaments fabricated by a chemical vapor deposition (CVD) method, Wilke *et al.*[4] showed that for carbon levels below 8%, the transition temperature is depressed by about 0.5 K/% C and $H_{c2}(0)$ is increased by about 2.5 T/% C, achieving upper critical fields in excess of 30 T at 4.2 K. Senkowicz *et al.*[5] have reported that milling C with MgB_2 can produce $H_{c2}(0)$ in excess of 32 T and critical current density approaching 10^6 A/cm^2.

Although carbon doping can significantly increase the upper critical field of MgB_2, and thus improve the $J_c(H)$ behavior at high field, however, the critical current density J_c of MgB_2 bulks sintered at ambient pressure is still inferior to the conventional A15 compound superconductors and Nb–Ti due to a poor connection between grains and the lack of flux pinning centers in the materials. It is expected that the pinning behavior in carbon-doped MgB_2 may be further improved if its microstructure can be improved. Ti may be a good candidate for this purpose since doping Ti in MgB_2 could highly improve the critical current density of MgB_2 in low field by controlling the microstructure of MgB_2.[6,7] Therefore, it is very possible to improve both H_{c2} and J_c of MgB_2 simultaneously by concurrently doping carbon and Ti, thus further improving its performance, especially in the higher magnetic field regime. However, until now, not much work has been done except the report by Wilke *et al.*,[8] who has shown that the addition of C to raise H_{c2} and the addition of Ti to form precipitate pinning centers are roughly independently of one another for their samples, prepared by a CVD method. Unfortunately, the J_c value achieved in their samples was relatively low due to some unknown reason.

[a)]Author to whom correspondence should be addressed; FAX: +86-28-87600184; electronic mail: yzhao@swjtu.edu.cn

Therefore, a more intensive study on the codoping effect of Ti and C is necessary to further improve the J_c of MgB_2 and to clarify the mechanism behind.

In this work, we intend to study the combination effect of C and Ti codoping in MgB_2 to determine whether bulk samples can be prepared with the combined benefits of both dopants by a simple *in situ* solid state reaction method which may be applicable in more feasible powder-in-tube process. Another purpose of this work is to probe the detailed mechanism of coaction of C and Ti doping of MgB_2.

II. EXPERIMENT

Experimental results showed that the optimum doping level of nanocarbon or carbon nanotubes (CNTs) in improving the J_c and H_{irr} of MgB_2 is 5 at. %.[9,10] In order to reveal the cooperative doping effect of Ti and C in MgB_2, $Mg_{1-x}Ti_xB_{2-y}C_y$ alloys of four typical compositions have been paid intensive attention. These samples include $Mg_{0.95}Ti_{0.05}B_2$ (denoted as Ti-doped), $MgB_{1.95}C_{0.05}$ (denoted as C-doped), $Mg_{0.95}Ti_{0.05}B_{1.95}C_{0.05}$ (denoted as C-Ti-doped), and undoped MgB_2 (denoted as undoped). Pellets of all these samples were synthesized by a solid state reaction, which has been previously described in detail, at ambient pressure with the starting materials of amorphous B powder (99.99%) and Mg powder (99.9%). The mean particle sizes of magnesium and boron were approximately 1 μm and 200 nm, respectively. Mixtures of magnesium, boron, graphite, and/or Ti powders were well ground in a glove box for 1 h and then uniaxially pressed into pellets of a diameter of 10 mm, sealed in iron tubes, and sintered at 800 °C for 1 h in flowing high purity Ar. Then the samples were quenched to room temperature in air. In order to increase the solubility of carbon in MgB_2 without increasing the reaction temperature and reaction time, high energy milling (HEM) was employed in the preparation of the samples. Except for the high energy milling of 1 h, the reaction temperature and reaction time for the samples prepared with HEM technique are the same as employed for other samples in this study.

Crystalline structure of the samples was investigated by powder x-ray diffraction (XRD) using an X'Pert MRD diffractometer with Cu $K\alpha$ radiation. The microstructure was analyzed by scanning electron microscope (SEM). All the samples were cut to the same size of $1.0\times1.5\times2.8$ mm^3 from as-sintered pellets. The magnetization of samples was measured over a temperature range of 5–50 K using a 9-T physical property measurement system (Quantum Design) in a time-varying magnetic field with sweep rate of 50 Oe/s and amplitude of up to 9 T. A magnetic J_c was derived from the width of the magnetization loop ΔM based on the extended Bean model: $J_c=20\Delta M/[a(1-a/3b)]$. The values of the irreversibility field H_{irr} were determined from the emerging point of the magnetization curves $M(T)$ measured in zero-field-cooling (ZFC) and field-cooling (FC) processes at various fields up to 7 T.

III. RESULTS AND DISCUSSION

Figure 1 shows the temperature dependence of the ZFC magnetization $M(T)$ measured under 50 Oe for the typical

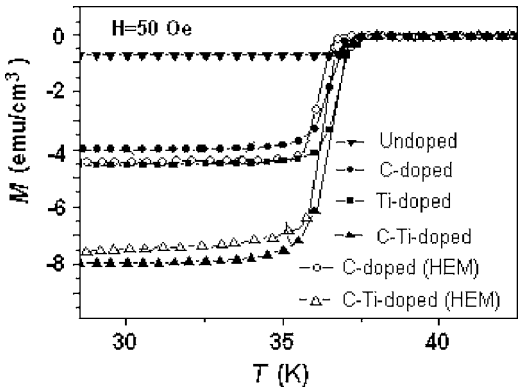

FIG. 1. The temperature dependent magnetization (ZFC) at 50 Oe for the undoped, Ti-doped, C-doped, and C–Ti-doped samples.

samples. All of these samples show a sharp superconducting transition, indicating a good quality and uniformity of their superconducting properties. For the undoped and Ti-doped samples, their T_c values are almost the same, about 37.8 K. This is consistent with previously reported results that doping Ti did not suppress the superconducting transition. For the samples doped with carbon including $MgB_{1.95}C_{0.05}$ and $Mg_{0.95}Ti_{0.05}B_{1.95}C_{0.05}$, T_c is depressed by 0.6 K for the samples without HEM, but by 1.3 K for those with HEM, compared to the T_c of carbon-free samples. The suppression of T_c can be attributed to the carbon doping since it directly depresses the superconductivity of MgB_2,[4] thus indicating that C has entered into MgB_2 lattice. According to the report of Wilke *et al.*,[4] that 5% C substitution will depress T_c from 39.2 to 36.7 K and raise $H_{c2}(T=0)$ from 16.0 to 26 T, the real doping level of carbon in our sample is deduced to be about 1.2% for the samples without HEM, but 2.5% for the samples with HEM, much lower than the nomination doping level of 5%. The results indicate that although the HEM is helpful for the increase of solubility of carbon in MgB_2, the carbon substitution reaction in these samples remains incomplete.

Figure 2 shows the typical magnetization hysteresis loops measured at 20 K for the undoped, Ti-doped, and C-Ti-doped MgB_2 samples (inset of Fig. 2) and the $J_c(H)$ curves for the typical samples at $T=20$ K. Magnetization hysteresis loops at 10 and 5 K are also measured and the general behaviors are similar to those at 20 K, except the occurrence of flux jumps at low fields. In this study, the focus will be the improvement of superconducting performance at 20 K because, at this temperature, the conventional superconductors, such as Nb_3Sn and Nb–Ti alloy, can no longer be used due to a lower T_c. For the undoped MgB_2, magnetization hysteresis loop is relatively narrow and small, suggesting a relatively low J_c and a low irreversibility field H_{irr}. After it was doped with Ti, the loop width, $\Delta M=|M^+(H)-M^-(H)|$ [where $M^+(H)$ and $M^-(H)$ are the magnetizations measured in the ascent and descent of the applied field, respectively], is significantly enlarged at low fields. However, the loop width decreases rapidly with increasing the applied magnetic field, suggesting a degradation of the flux pinning in the magnetic field. By further doping C in Ti-doped MgB_2, the rapid decrease of ΔM is suppressed.

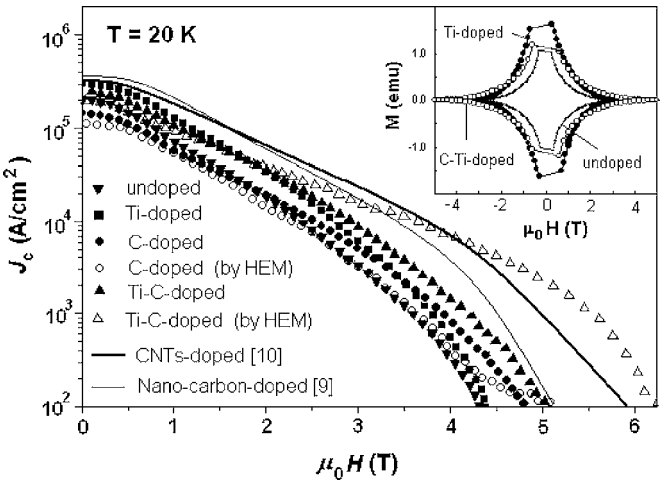

FIG. 2. $J_c(H)$ behavior at $T=20$ K for the undoped, Ti-doped, C-doped, and C–Ti-doped samples. For the sake of comparison, the J_c results of nanocarbon-doped MgB_2 (Ref. 9) and CNT-doped MgB_2 are plotted in the figure. Inset: Magnetization hysteresis loops at $T=20$ K for undoped, Ti-doped, and C–Ti-doped samples.

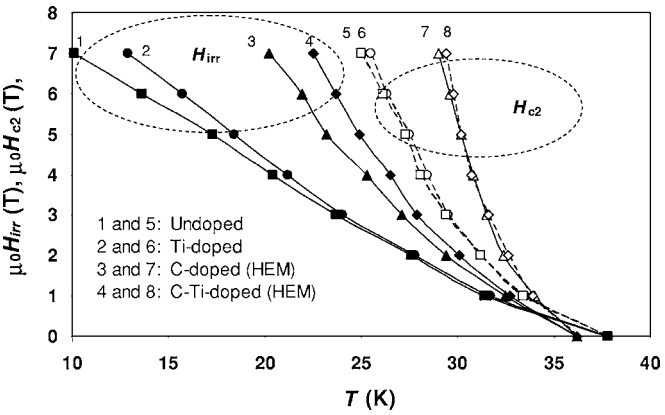

FIG. 3. Temperature dependence of H_{irr} and H_{c2} for the samples studied in this work.

As shown in the main panel of Fig. 2, the in-field critical current densities were enhanced by Ti doping, particularly in lower fields. At 20 K, the maximum zero field value $J_c(0)$ was achieved in $Mg_{0.95}Ti_{0.05}B_2$ sample, a J_c value in self-field at 20 K was improved from 2.1×10^5 A/cm^2 of non-doped sample to 3.1×10^5 A/cm^2. This result is consistent with our previous report on Ti-doped MgB_2 bulk superconductor, where $J_c(0)$ was improved by refining MgB_2 grains and forming a strongly coupled nanoparticle structure.[7] On the other hand, the addition of carbon does degrade J_c at low field, maybe due to the reduction in T_c. However, the crucial result is that the field dependence of J_c flattens significantly in the C-doped sample, with a significant improvement of irreversibility field H_{irr}. This slower depression of J_c by the field suggests that C doping has the benefit of improving the $J_c(H)$ behavior of MgB_2 in higher fields, which is consistent with the result that carbon doping enhances the upper critical field of MgB_2.

The most striking feature shown in Fig. 2 is that the C-Ti-doped sample exhibited the combined benefits of C and Ti. The J_c values of this sample is lower than that of Ti-doped sample in magnetic field from 0 to 2 T, but in higher magnetic fields (>2 T), its J_c is significantly improved and much higher than the J_c of Ti-doped sample. Accordingly, the irreversibility field is also significantly improved. What is more, this sample showed a better in-field J_c than carbon-doped samples, including nanocarbon-doped MgB_2 (Ref. 9) and CNT-doped MgB_2,[10] in the high magnetic field region. At temperature of 20 K, the J_c reaches 1×10^4 A/cm^2 in 4 T, and 4×10^3 A/cm^2 in 5 T; and the irreversibility field determined from the closure of hysteresis loops with a criterion of 10^2 A/cm^2 exceeds 6 T. This is one of the best values for MgB_2 at 20 K. The improvement of J_c and pinning behavior at 10 and 5 K are also observed. Our results clearly show that concurrently doping Ti and C in MgB_2 is a feasible and effective route to further improve the superconducting performance of MgB_2, especially at higher temperatures (~20 K) and in higher fields (>3 T).

The above-mentioned results suggest that the doping effects of C and Ti to improve the superconducting performance are largely cooperative. To explore the mechanism behind, the irreversibility lines $H_{irr}(T)$ and the behavior of upper critical field $H_{c2}(T)$ are investigated. Figure 3 shows the results of $H_{irr}(T)$ and $H_{c2}(T)$, which are obtained from the temperature dependence of the magnetization measured in the ZFC and FC processes in various applied fields. The $H_{c2}(T)$ is determined from the point at which the magnetization starts to deviate from the normal state linear background, while the $H_{irr}(T)$ line is determined by taking the deviating point between ZFC-FC $M(T)$ curves with a criterion of $\Delta M_{ZFC-FC}=10^{-4}$ emu. It can be seen from Fig. 3 that the irreversibility field is improved by doping Ti and/or carbon. The level of H_{irr} improved by these dopants is successively the Ti-doped, C-doped, and C-Ti-doped ones. In addition, it is noted that although doping Ti leads to an improvement of H_{irr}, however, it almost has no effect on the improvement of H_{c2}. Different from doping Ti, doping C does improve both H_{irr} and H_{c2}. What is important is that the C-Ti-doped sample exhibits the best H_{irr} and H_{c2} amongst the samples in the present study, which is consistent with the results of J_c as shown in Fig. 2.

The effects of doping Ti and/or C in MgB_2 on the J_c, H_{irr}, and H_{c2} are summarized in Table I. As revealed by XRD analyses (see Fig. 4), Ti does not enter the lattice of MgB_2, thus having almost no effect on intrinsic properties of MgB_2, such as T_c and H_{c2}. By improving the microstructure,[7] doping Ti enhances the grain boundary pinning in MgB_2, consequently improving J_c and H_{irr}. Because the H_{c2} of MgB_2 is relatively low, the improvement of J_c by doping Ti is mainly limited in the low field, and the improvement of H_{irr} by doping Ti is not very significant. Different from doping Ti, doping C introduces impurity scattering centers in the lattice of MgB_2, leading to a decrease of T_c but an increase of H_{c2}. Therefore, doping C slightly decreases J_c in low fields due to the suppression of superconductivity. However, because of the enhancement of H_{c2}, the irreversibility field is raised, and consequently, the J_c is improved at high fields, suggesting that a high H_{c2} is important for the enhancement of J_c at high fields. For concurrently doping C and Ti, carbon-doping-induced depression of J_c in low fields has

TABLE I. The summary of doping effects of C and Ti on MgB_2.

	Effect on T_c	Effect on H_{c2}	Effect on H_{iir}	Effect on J_c	Mechanism
Doping Ti	No effect	No effect	Slightly increased	Significantly improved in lowfields	Enhancement of flux pinning
Doping C	Moderately decreased	Significantly increased	Significantly increased	Slightly depressed in low field, but improved in high fields	Enhancement of impurity scattering for charge carriers
Doping C and Ti	Moderately decreased	Significantly increased	Significantly increased	Significantly improved in whole range of fields	Enhancement of both flux pinning and impurity scattering

been compensated by doping Ti. Moreover, the increase of H_{c2} by doping C and the increase of pinning center by doping Ti have largely cooperated, which leads to a significant improvement of the high-field J_c and the H_{irr}.

Figure 4 shows results of high resolution x-ray diffraction measurements for the samples studied in this work. MgO impurity phase was detected in all of these samples. However, no evidence of TiC or other Ti–C–B composites are present in $Mg_{0.95}Ti_{0.05}B_{1.95}C_{0.05}$ sample, indicating that the addition of Ti may act independently of C. This viewpoint was confirmed by further analysis shown below.

Figure 5 shows an expanded view of the (100) peak of investigated samples. The (002) peak is omitted. Within the accuracy of these measurements, there is no shift in the (002) peak of the samples, suggesting no measurable change in the *c*-axis lattice parameter. The (100) peak of $MgB_{1.95}C_{0.05}$ sample and $Mg_{1.95}Ti_{0.05}B_{1.95}C_{0.05}$ nearly overlapped, shifting out from the pure MgB_2 peak and $Mg_{0.95}Ti_{0.05}B_2$ by about 0.12°, thus indicating a decrease of *a*-axis lattice. This result seems to suggest that the addition of Ti to the C-doped MgB_2 does not reduce the amount of C in the MgB_2 lattice. In addition to shortening the electronic mean free path, disorder induced by carbon impurity in MgB_2, given its two-gap superconductivity, might manifest itself as an increase of H_{c2} by selective tuning of impurity scattering. The same amount of C in B site therefore should be responsible for the excellent J_c at high fields for both $MgB_{1.95}C_{0.05}$ and $Mg_{0.95}Ti_{0.05}B_{1.95}C_{0.05}$. What is more, a phenomenon that is worth noting is that the full width at half maximum (FWHM) of (100) peak for the carbon-containing samples is larger than that for the carbon-free samples. Because (100) peak reflects the lattice constant of the honeycomb boron sheet, the broadening of this peak may suggest the occurrence of some distortion of the sheet. This result is consistent with the report of Yamamoto *et al.*[11] who observed that the FWHM of (110) peak, which also corresponds to the distortion of honeycomb boron sheet, has a positive correlation with the H_{irr} of MgB_2, that is, H_{irr} increases with increasing FWHM of (110) peak. Because the honeycomb boron sheet takes the responsibility of superconductivity in MgB_2, a distortion of the sheet may result in the imperfection-induced scattering for charge carriers, thus enhancing H_{c2}. Therefore, the underpinning mechanism behind the correlation between FWHM of (110) peak and H_{irr} should be the impurity-induced enhancement of H_{c2}.

Figure 6 shows typical SEM photomicrographs illustrating the structure of the sintered bulk of $Mg_{0.95}Ti_{0.05}B_2$, $MgB_{1.95}C_{0.05}$, and $Mg_{0.95}Ti_{0.05}B_{1.95}C_{0.05}$. All these samples were sintered at 800 °C for 1 h, followed by quenching in air. As revealed by the insets, the $Mg_{0.95}Ti_{0.05}B_2$ and $Mg_{0.95}Ti_{0.05}B_{1.95}C_{0.05}$ had a very dense structure, whereas the $MgB_{1.95}C_{0.05}$ sample was porous, with significant amount of voids in micron size, resulting in a rather low bulk density of 1.33 g cm^{-3}, which is almost half of the theoretical density of MgB_2, 2.62 g cm^{-3}. This result indicated that Ti doping served as sintering aid to form a strongly grain connected

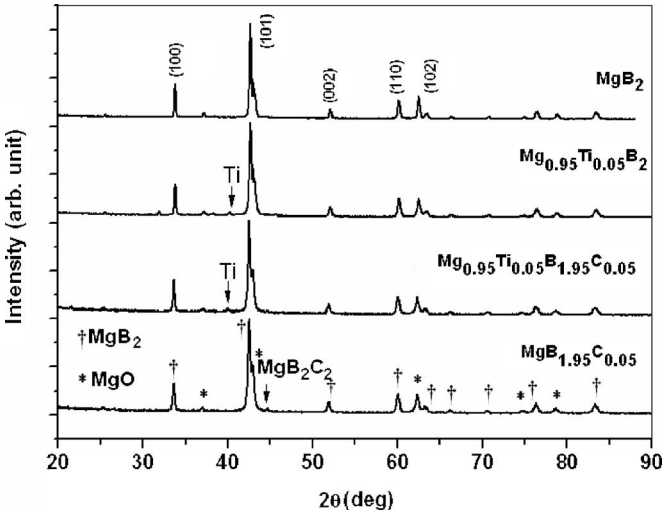

FIG. 4. XRD patterns for the samples studied in this work. From top to bottom: MgB_2, $Mg_{0.95}Ti_{0.05}B_2$, $Mg_{0.95}Ti_{0.05}B_{1.95}C_{0.05}$, and $MgB_{1.95}C_{0.05}$.

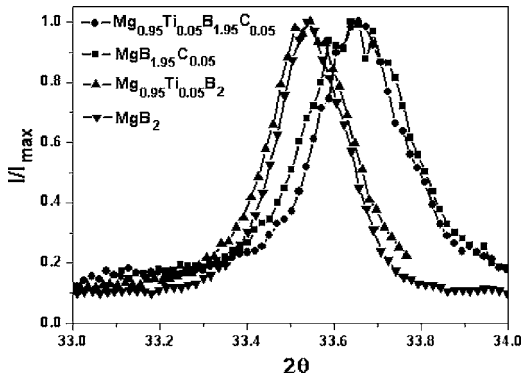

FIG. 5. The (100) Bragg reflections for the MgB_2 samples studied in this work.

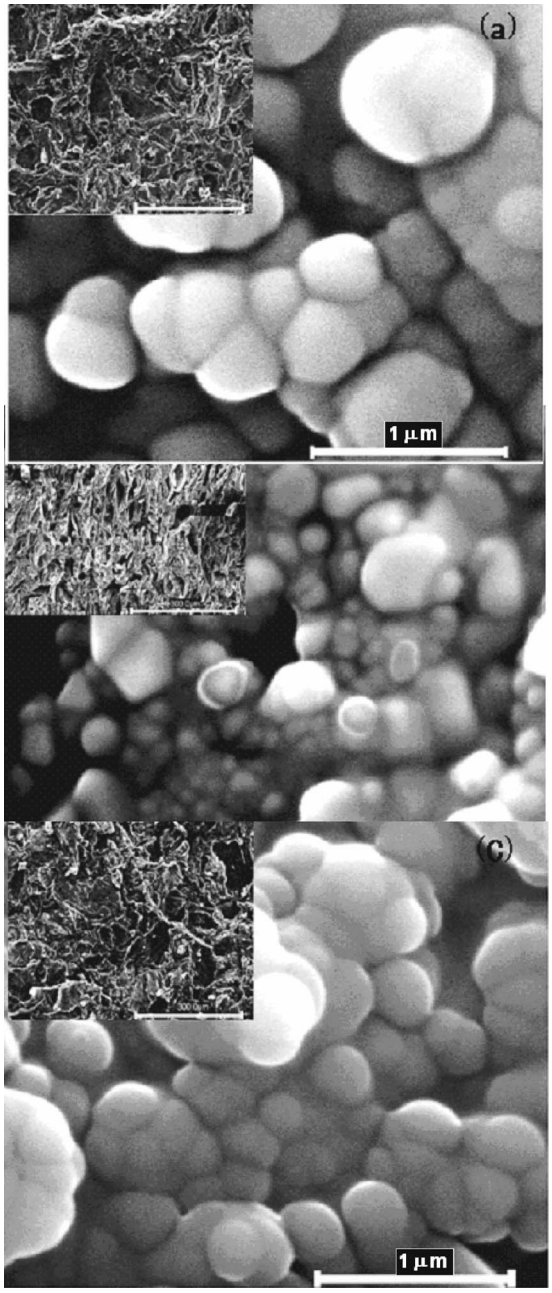

FIG. 6. Typical SEM images for MgB_2 bulk doped with (a) Ti, (b) C, and (c) Ti and C. The scale bars are 1 μm in length. The inset of each figure was the secondary electron image of the fractured surface with a lower magnification of 200, in which the scale bars are 300 μm.

network structure. This result is consistent with our previous report, where Ti doping resulted in an excellent grain connection and extremely high density. Densification would increase the effective cross-sectional area for the transportation of supercurrent in the samples. On the other hand, the C doping showed no densification effect. Thus, Ti doping into $Mg(B_{1-x}C_x)_2$ is helpful to form the strongly grain connected network structure and increase the effective current pass, which is beneficial in enhancing J_c.

Furthermore, as revealed by Fig. 6, all three samples are typical nanocrystalline MgB_2 bulk superconductors with a grain size around 10–300 nm. It should be noted that though the average grain size in $MgB_{1.95}C_{0.05}$ was the smallest, there are a significant amount of pores about 200–500 nm in size in C-doped MgB_2. Moreover, the size of MgB_2 grains was found to be rather inhomogeneous, with a wide size distribution, ranging from 10 to 500 nm in diameter. In contrast to this structure, the $Mg_{0.95}Ti_{0.05}B_{1.95}C_{0.05}$ bulk material mainly consists of uniform spherical grains about 200–300 nm in size. Thus, Ti doping into $MgB_{1.95}C0.05$ has another effect: uniform grains. Therefore, besides a strongly grain coupled network, grain homogeneity may be responsible for the improved J_c at low fields for C-Ti-doped MgB_2. Therefore, the concurrent doping of C and Ti is also superior, in improving the microstructure of MgB_2, to the carbon-only doping.

IV. CONCLUSION

The present work shows that codoping C and Ti is a promising way to fabricate high density nanocrystalline MgB_2 bulk material with excellent values of $J_c(T)$ and $H_{irr}(T)$. The addition of C and Ti was found to be largely cooperative in improving the superconducting properties of MgB_2 material. The addition of Ti into C-doped MgB_2 was found to result in a strongly grain connected network structure and high grain homogeneity, both of which are considered to enhance J_c at low fields. On the other hand, Ti doping did not reduce the amount of C in the MgB_2 lattice. Thus, the carbon in $Mg_{1-x}Ti_xB_{2-y}C_y$ seems to play the same role, as in $MgB_{2-x}C_x$, in improving the $H_{c2}(T)$ by shortening the mean free length of electron, or selective tuning of impurity scattering of π and σ bands according to the two-gap model. Finally, it should be pointed out that the high $H_{c2}(T)$ is of vital importance for improving J_c in the high-field region.

ACKNOWLEDGMENTS

The authors are grateful for the financial support of the Australian Research Council (under Contract Nos. DP0559872 and DP0452522) and UNSW (Goldstar Awards). This work was also supported by the Natural Science Foundation of China (under Contract Nos. 50372052 and 50588210).

[1] A. Gurevich, Phys. Rev. B **67**, 184515 (2003).
[2] A. Gurevich *et al.*, Supercond. Sci. Technol. **17**, 278 (2004).
[3] V. Braccini *et al.*, Phys. Rev. B **71**, 012504 (2005).
[4] R. H. T. Wilke, S. L. Bud'ko, P. C. Canfield, and D. K. Finnemore, Phys. Rev. Lett. **92**, 217003 (2004).
[5] B. J. Senkowicz, J. F. Giencke, S. Patnaik, C. B. Com, E. E. Hellstrom, and D. C. Larbalestier, Appl. Phys. Lett. **86**, 202502 (2005).
[6] Y. Zhao *et al.*, Appl. Phys. Lett. **79**, 1154 (2001).
[7] Y. Zhao, D. X. Huang, Y. Feng, C. Cheng, T. Machi, N. Koshizuka, and M. Murakami, Appl. Phys. Lett. **80**, 1640 (2002).
[8] R. H. T. Wilke *et al.*, Physica C **418**, 160 (2005).
[9] S. Soltanian, J. Horvat, X. L. Wang, P. Munroe, and S. X. Dou, Physica C **390**, 185 (2003).
[10] S. X. Dou, W. K. Yeoh, J. Horvat, and M. Ionescu, Appl. Phys. Lett. **83**, 4996 (2003).
[11] A. Yamamoto, J. Shimoyama, S. Ueda, Y. Katsura, I. Iwayama, S. Horii, and K. Kishio, Appl. Phys. Lett. **86**, 212502 (2005).